A Diode Laser-Grating Study of the $\nu_2 + \nu_5$ Band of C_2D_2

S. Alanko, R. Paso, and R. Anttila
Department of Physics, University of Oulu, Oulu, Finland

Z. Naturforsch. **42 a,** 1247–1252 (1987); received July 11, 1987

The region of the $\nu_2 + \nu_5$ band of deuterated acetylene C_2D_2 around 2305 cm^{-1} has been studied using a diode laser-grating spectrometer. The grating spectrum covered the whole range of the band. The structure of the Q branch as well as the Q branches of the hot bands $\nu_2 + 2\nu_5 \leftarrow \nu_5$ and $\nu_2 + \nu_4 + \nu_5 \leftarrow \nu_4$ together with some special parts have been investigated with the diode laser, too. Molecular constants for the $\nu_2 + \nu_5$ band with small improvements in the ground state constants are presented. The hot bands were analyzed by taking the l-resonances into account.

Key words: Diode laser, Infrared spectrum, Rotation-vibration spectrum, Deuteroacetylene, l-resonance.

1. Introduction

Diode lasers are especially suitable for spectroscopic problems where high resolution is necessary to resolve dense structures but where at the same time it is not so important to scan continuously wide wavenumber ranges. The study of the Q branches in the spectra of linear molecules forms an example of such problems and there are numerous diode laser investigations of this type. The operating region of our diode laser spectrometer is suited for the study of the $\nu_2 + \nu_5$ band of deuterated acetylene. So we determined to continue the series of acetylene studies in our laboratory, see [1] and the references cited there. Especially we wanted to make a comparison with the ν_5 band and with the hot bands accompanying it [2].

2. Experimental

The measurements were performed using the diode laser-grating spectrometer at the University of Oulu [3, 4]. The grating spectrometer is of the Littrow-type having a focal length of 4.5 m. The whole band was recorded with this apparatus at a resolution of 0.06 cm^{-1}. The central part of the spectrum is illustrated in Figure 1. Simultaneously with the spectrum an interferometric scale was registered [4]. The separation of the fringes produced by He-Ne laser light was about 0.007 cm^{-1}. With the aid of this scale the spectrum was calibrated by using CO_2 absorption peaks [5]. The sample gas from Merck Sharp & Dohme was in a White-type cell giving an absorption path length of 15 m. The pressure was 20 Torr.

The regions of the Q branches in Fig. 1 together with several additional parts were scanned with the diode laser spectrometer. The laser diode and its cold head and control systems are from Laser Analytics Inc. The grating instrument mentioned above was applied to isolate the modes of the laser.

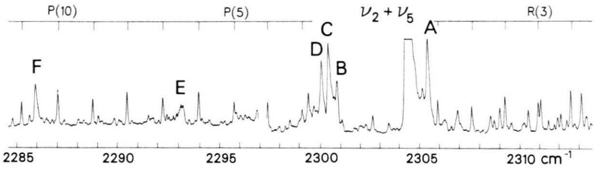

Fig. 1. Overall grating spectrum with P and R line assignments of the central part of the $\nu_2 + \nu_5$ band of C_2D_2. The hot band Q branches are indicated as follows: A, $\nu_2 + 2\nu_5(\Delta_g) \leftarrow \nu_5(\pi_u)$; B, $\nu_2 + 2\nu_5(\Sigma_g^+) \leftarrow \nu_5(\pi_u)$; C, $\nu_2 + \nu_4 + \nu_5(\Sigma_u^-) \leftarrow \nu_4(\pi_g)$; D, $\nu_2 + \nu_4 + \nu_5(\Delta_u) \leftarrow \nu_4(\pi_g)$; E, $\nu_2 + \nu_4 + \nu_5(\Sigma_u^+) \leftarrow \nu_4(\pi_g)$. The Q branch of $\nu_2 + \nu_5$ of $D^{12}C^{13}CD$ is marked by F. Experimental conditions: path length 15 m, sample pressure 2700 Pa (20 Torr), room temperature.

Reprint requests to S. Alanko, Department of Physics, University of Oulu, SF-90570 Oulu, Finland.

0932-0784 / 87 / 1100-1247 $ 01.30/0. – Please order a reprint rather than making your own copy.

This double use of the grating device makes it possible to relate the laser scans to the overall spectrum from the knowledge of grating settings. This speeds up both the measurements and the assignments of the diode laser spectra. Calibration was done by using a 75 mm long germanium etalon (free spectral range 0.0162 cm^{-1}) and CO_2 absorption peaks. The spectral pieces together with the scale were generally recorded twice: with and without a CO_2 cell in the sample beam. The sample was in the same White-type cell as above but the pressures were now varied from about 0.5 Torr to 20 Torr.

3. The Band $\nu_2 + \nu_5$

The grating spectrum covered the band from P(32) to R(28). The observed 47 P and R lines were fitted to a third order polynomial and the standard deviation was about 0.003 cm^{-1}. This fit gave starting values for the band parameters. The *Q* branch in the grating spectrum in Fig. 1 appears with a sharp lower edge. It is degrading to higher wavenumbers but no line structure is resolved.

The composite spectrum over the *Q* branch region formed from diode laser recording pieces is presented in Figure 2. This figure includes measurements under two different pressures. When using a still smaller pressure the low *J* part could be resolved until $J = 4$ although in the beginning only the stronger lines (*J* even) were detected. The observed line positions are presented in Table 1. All the *Q* lines are from the diode laser measurements whereas P and R lines are mostly from the grating spectrum.

When starting the analysis we tried to improve the ground state constants B_0 and D_0. We fitted together the ground state combination differences from [2] and from this work. The results are given in the beginning of Table 2. The error limits are slightly narrower than those in [2].

In the further analysis of the $\nu_2 + \nu_5$ band the ground state constants were fixed. The P, Q and R lines were analyzed simultaneously. For the upper state $\nu_2 + \nu_5$ the term values

$$T_{25} = E_{25} - B_{25} - D_{25} + (B_{25} \pm \tfrac{1}{2} q_5^{25} + 2 D_{25}) J(J+1) - (D_{25} \mp \tfrac{1}{2} \mu_5^{25}) [J(J+1)]^2 \qquad (1)$$

were used. In (1) E_{25} represents purely vibrational energy, B_{25} and D_{25} are the rotational and centrifugal distortion constants, q_5^{25} is the *l*-doubling constant whose rotational dependence is described by μ_5^{25} [1]. We use the notations q_5^{25} and μ_5^{25} to indicate that the *l*-doubling constants q_5 and μ_5 have an expansion as a function of the vibrational quantum numbers, i.e. q_5 and μ_5 at the state $\nu_2 + \nu_5$ are different from q_5 and μ_5 at ν_5. The upper signs are

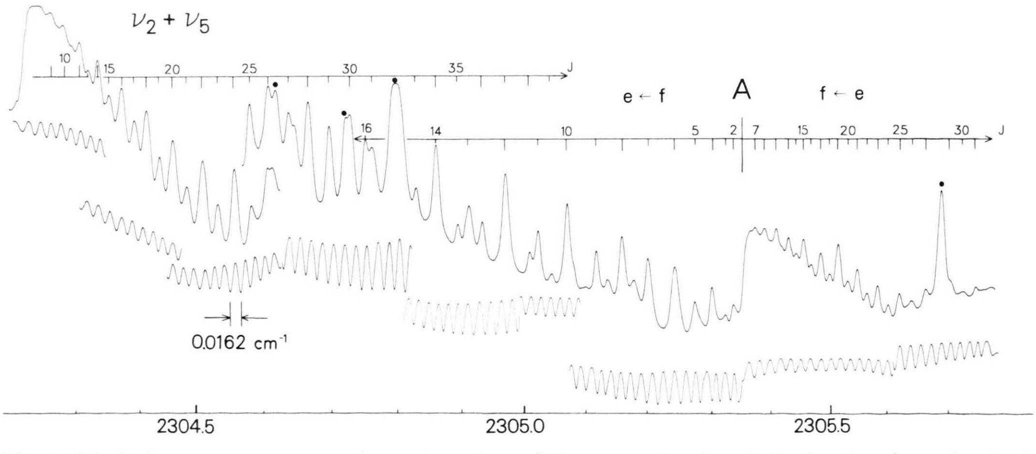

Fig. 2. Diode laser spectrum over the Q branches of the $\nu_2 + \nu_5$ band and the hot band $\nu_2 + 2\nu_5 (\Delta_g) \leftarrow \nu_5 (\pi_u)$ (A in Figure 1). The lines at 2305.14 cm^{-1} and 2305.18 cm^{-1} which do not belong to any Q branch are hot band R lines. The lines marked with dots are due to CO_2. Experimental conditions: path length 15 m, pressure 200 Pa in the region of the strongest absorption below 2304.6 cm^{-1} and 1000 Pa elsewhere. The interference fringes produced by the Ge-etalon are also visible.

Table 1. Observed line positions (cm^{-1}) in the band $\nu_2 + \nu_5$ of C_2D_2. The wave numbers based on diode laser measurements are indicated by *D*. The differences O−C are given in 10^{-4} cm^{-1}.

J	P(*J*)	O−C	Q(*J*)	O−C	R(*J*)	O−C
0					2305.9224	−2 D
1						
2	2300.8339	−16 D			2309.2857	−9 D
3	2299.1288	1 D			2310.9615	13
4			2304.2438	1 D	2312.6246	−37
5						
6	2293.9730	−31	2304.2567	5 D	2315.9471	−6
7	2292.2465	−13 D			2317.5974	−15
8	2290.5173	32	2304.2737	7 D		
9	2288.7803	52			2320.8894	50
10	2287.0308	0 D	2304.2958	14 D	2322.5162	−24
11	2285.2793	−18	2304.3058	−10 D		
12	2283.5276	15	2304.3205	4 D	2325.7702	4
13	2281.7676	17	2304.3348	2 D	2327.3883	15
14	2279.9998	−6 D	2304.3506	4 D	2328.9952	−28
15	2278.2274	−23 D	2304.3677	9 D		
16	2276.4548	11 D	2304.3849	4 D	2332.2053	23
17	2274.6720	−5 D	2304.4038	6 D	2333.7932	−35
18	2272.8865	4	2304.4231	2 D	2335.3850	5
19	2271.0903	−43	2304.4441	4 D	2336.9705	40
20	2269.2981	2	2304.4657	3 D	2338.5474	49
21	2267.4979	19	2304.4886	5 D	2340.1162	36
22	2265.6884	−6	2304.5122	4 D	2341.6829	62
23	2263.8778	9	2304.5367	3 D	2343.2415	67
24	2262.0589	−8	2304.5618	−3 D	2344.7956	87
25			2304.5883	−3 D		
26	2258.4066	−34	2304.6152	−7 D	2347.8794	65
27	2256.5682	−94	2304.6443	1 D	2349.4098	29
28			2304.6727	−7 D		
29			2304.7031	−3 D		
30	2251.0423	−77	2304.7334	−9 D		
31			2304.7644	−15 D		
32	2247.3376	−24	2304.7993	10 D		
33			2304.8311	−4 D		
34						
35			2304.9000	−0 D		
36			2304.9354	1 D		
37						
38			2305.0093	15 D		
39			2305.0446	−5 D		

Table 2. Results (in cm^{-1}) from the analysis of the $\nu_2 + \nu_5$ band of C_2D_2 [a].

$B_0 = 0.847875(8)$ [b]
$D_0 = 0.8011(28) \times 10^{-6}$ [b]
$E_{25} = 2305.07917(27)$
$B_{25} - B_0 = -1.0916(17) \times 10^{-3}$
$q_5^{25} = -3.3144(25) \times 10^{-3}$
$D_{25} - D_0 = 0.0190(23) \times 10^{-6}$
$\mu_5^{25} = 0.0214(43) \times 10^{-6}$

---

[a] The error limits are one standard deviation in the units of the last digit given.

[b] Obtained from the simultaneous fit of ground state combination differences from this work and [2].

Table 3. Results (in cm^{-1}) from the analysis of the $\nu_2 + \nu_5$ band of $D^{12}C^{13}CD$.

$B_0 = 0.83305$ Ref. [2]
$D_0 = 0.70 \times 10^{-6}$ Ref. [2]
$E_{25} = 2286.7208(9)$
$B_{25} - B_0 = -1.103(9) \times 10^{-3}$
$q_5^{25} = -3.078(13) \times 10^{-3}$
$D_{25} - D_0 = 9.0(28) \times 10^{-9}$
$\mu_5^{25} = 0$ fixed

Number of lines 32
Std. dev. 0.0018

valid for the e-levels which are reached by the P and R transitions, the lower signs apply for the f-levels.

In the fit the diode laser lines had a weight of 20 and the lines from the grating spectrum had a weight of 1 according to estimated measurement accuracies. The rms value for the residuals in the whole fit was 0.0012 cm^{-1} whereas for those 31 Q lines which all are from diode laser spectra it was 0.0007 cm^{-1}. The molecular parameters from the analysis are given in Table 2. The result for the difference $B_{25} - B_0$ is near to $-(\alpha_2 + \alpha_5) = -0.996 \times 10^{-3}\,\mathrm{cm}^{-1}$ [2, 6]. The negative value for the *l*-doubling constant together with what has been said above indicates that the f-levels are higher than e-levels. This is coherent with the situation in the fundamentals of acetylenes [1, 7]. Our numerical value of q_5^{25} is slightly larger than q_5 for the $v_5 = 1$ state [2, 8]. The vibrational energy when combined with v_2 [6] and v_5 [2] leads to the anharmonicity constant $x_{25} = 1.647\ \mathrm{cm}^{-1}$.

The Q branch marked with F in Fig. 1 is represented in detail in Figure 3. It could not be assigned to any hot band. As there is no intensity variation discernible between adjacent lines we interpreted the Q branch to be that of the $\nu_2 + \nu_5$ band of the isotopomer $D^{12}C^{13}CD$. Altogether 26 Q lines could be assigned to J values between 7 and 36. In addition six P and R lines were found. The analysis was performed in a way analogous to that in the case of the main band. The ground state values B_0 and D_0 were fixed according to [2]. The results are given in Table 3. The vibrational isotopic shift from Tables 2 and 3 is 18.36 cm^{-1}. This is well in agreement with 17.49 cm^{-1}, the sum of the corresponding isotopic effects in ν_2 [6] and in ν_5 [2]. This confirms our interpretation. The results for $B' - B''$ and for q_5^{25} are reasonably near to those for $^{12}C_2D_2$.

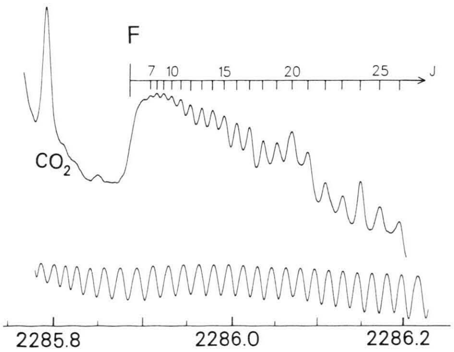

Fig. 3. Diode laser spectrum of the Q branch of the $\nu_2 + \nu_5$ band of $D^{12}C^{13}CD$. (F in Fig. 1). Experimental conditions as in Fig. 2 (higher pressure).

4. Hot Bands

In the grating spectrum several additional Q branches were seen (A–E in Figure 1). Starting from the hot band structure around ν_5 [2] and by using x_{25} from above and x_{24} given by Kostyk and Welsh [6] the Q branches could be assigned to the transitions originating from the levels $v_4 = 1$ and $v_5 = 1$. Although the Q branch lines were not resolved, additional information could be drawn from the widths and degradation directions of the Q branches. This knowledge confirmed the assignments. Neither P nor R lines belonging to the hot bands were detected.

When studying the hot band Q branches with the diode laser, single rotational lines were resolved in all of them. Some P and R lines were observed, too. The numbers of P, Q and R lines in different hot bands are compiled in Table 4. The small number of R lines is due to the fact that we could not make laser measurements above 2310.6 cm^{-1}. When thinking at the analysis it is very important that we have P and R lines, too. There is a danger for malassignments if only Q lines are used and the structure is not resolved from the beginning.

(i) *The hot bands* $\nu_2 + 2\nu_5 \leftarrow \nu_5$

The vibrational state $\nu_2 + 2\nu_5$ includes the Δ_g and Σ_g^+ components. The transition $\nu_2 + 2\nu_5(\Delta_g) \leftarrow \nu_5(\Pi_u)$

Table 4. Number of assigned lines in the hot bands $\nu_2 + 2\nu_5 \leftarrow \nu_5$ and $\nu_2 + \nu_4 + \nu_5 \leftarrow \nu_4$ of C_2D_2.

Upper state	Number of Q lines	Number of P, R lines
$\nu_2 + 2\nu_5(\Sigma_g^+)$	19	10.2
$\nu_2 + 2\nu_5(\Delta_g^e)$	14	8.2
$\nu_2 + 2\nu_5(\Delta_g^f)$	24	10.2
$\nu_2 + \nu_4 + \nu_5(\Sigma_g^+)$	20	6.2
$\nu_2 + \nu_4 + \nu_5(\Sigma_g^-)$	11	8.2
$\nu_2 + \nu_4 + \nu_5(\Delta_g^e)$	21	8.2
$\nu_2 + \nu_4 + \nu_5(\Delta_g^f)$	17	11.1

Table 5. Results from the analysis of the hot bands $\nu_2 + 2\nu_5 \leftarrow \nu_5$ and $\nu_2 + \nu_4 + \nu_5 \leftarrow \nu_4$ of C_2D_2.

Constrained lower state constants in cm^{-1} [1]			
$B_5 =$	0.849998	$B_4 =$	0.849929
$D_5 =$	0.817×10^{-6}	$D_4 =$	0.828×10^{-6}
$q_5 =$	-3.275×10^{-3}	$q_4 =$	-3.245×10^{-3}
$\mu_5 =$	0.031×10^{-6}	$\mu_4 =$	0.023×10^{-6}
Constants for $\nu_2 + 2\nu_5$ in cm^{-1}		Constants for $\nu_2 + \nu_4 + \nu_5$ in cm^{-1}	
$E_{255} - E_5 =$	2300.0604(4)	$E_{245} - E_4 =$	2299.2821(4)
$g_{55} =$	1.96041(12)	$g_{45} =$	3.3080(4)
$B_{255} - B_5 =$	$-1.057(4) \times 10^{-3}$	$B_{245} - B_4 =$	$-1.155(3) \times 10^{-3}$
$\gamma^{55} =$	$-0.0403(1) \times 10^{-3}$	$\gamma^{45} =$	$-0.072(7) \times 10^{-3}$
$q_5^{255} - q_5 =$	$-0.035(6) \times 10^{-3}$	$q_4^{245} - q_4 =$	$-0.184(9) \times 10^{-3}$
		$q_5^{245} =$	$-3.11(5) \times 10^{-3}$
$D_{255} - D_5 =$	$0.013(2) \times 10^{-6}$	$D_{245} - D_4 =$	$0.011(5) \times 10^{-6}$
$\mu_5^{255} =$	μ_5 fixed	$\mu_4^{245} =$	μ_4 fixed
		$r_{45}^0 =$	$-3.5450(5)$
		$r_{45}^j =$	$0.070(2) \times 10^{-3}$
Std. dev.	0.0014	Std. dev.	0.0019
Number of lines 91		Number of lines 109	

gives rise to a Q branch which has two components degrading to opposite directions, as can be seen in Figure 2. The lower frequency component $e \leftarrow f$ is broad and the lines are resolved from the very beginning but the tail is overlapped by the main band. The upper component $f \leftarrow e$ is much sharper. The observed intensity variation was useful when making the assignments.

In the Q branch $\nu_2 + 2\nu_5 (\Sigma_g^+) \leftarrow \nu_5 (\Pi_u)$ (B in Fig. 1) the lines were resolved from very low J values. In spite of the overlapping other Q branches, 19 lines could be assigned. There were some difficulties in finding suitable laser modes in this region.

The analysis of 91 lines in the hot bands $\nu_2 + 2\nu_5 (\Delta_g) \leftarrow \nu_5 (\Pi_u)$ and $\nu_2 + 2\nu_5 (\Sigma_g^+) \leftarrow \nu_5 (\Pi_u)$ was performed simultaneously. The lower state term values corresponding to that in (1) were used with fixed constants given in Table 5. For the upper state $\nu_2 + 2\nu_5$ the term values were calculated from the general expression

$$T_v = E_v + g_{tt'} l_t l_{t'} + (B_v + \gamma^{tt'} l_t l_{t'}) [J(J+1) - l^2] - D_v [J(J+1) - l^2]^2 . \qquad (2)$$

In the case of $\nu_s + 2\nu_5$ we have $t = t' = 5$ and $l = l_5 = \pm 2$ or 0. In the analysis it is essential to take into account the l-resonance, which causes remarkable shifts in $\nu_2 + 2\nu_5 (\Sigma_g^+)$ and in the e-component of $\nu_2 + 2\nu_5 (\Delta_g)$. The l-resonances have been thoroughly discussed by J. Hietanen in his thesis [1]. The coupling matrix elements are given by Pliva [7] and by Winnewisser and Winnewisser [9]. They can be written

$$\langle v_t, l_t | H'_2 | v_t, l_t \pm 2 \rangle = \frac{q_t^*}{4} \{(v_t \mp l_t)(v_t \pm l_t + 2) [J(J+1) - l(l \pm 1)] \times [J(J+1) - (l \pm 1)(l \pm 2)]\}^{1/2} , \qquad (3)$$

where in the case of the $\nu_2 + 2\nu_5$ state

$$q_t^* = q_5^{255} + \mu_5^{255} J(J+1) . \qquad (4)$$

The energies for the $\nu_2 + 2\nu_5$ state were obtained as the eigenvalues of 3×3 matrices for every J value. The resulting parameters are presented in Table 5.

(ii) *The hot bands* $\nu_2 + \nu_4 + \nu_5 \leftarrow \nu_4$

The hot bands starting from $v_4 = 1$ lead to the state $\nu_2 + \nu_4 + \nu_5$ which has the components Σ_u^+, Σ_u^- and Δ_u. The Q branches of the corresponding hot bands are marked with E, C and D in Figure 1. The lowest of these, E (Σ_u^+), has a broad structure which is well resolved with the laser. The Q branch C, that of $\nu_2 + \nu_4 + \nu_5 (\Sigma_u^-) \leftarrow \nu_4 (\Pi_g)$, is sharp and overlapped by other Q branches. The assignment of its blended structure was somewhat difficult and even in the final fit the deviations here remained larger than in the other Q branches. The Q branch of $\nu_2 + \nu_4 + \nu_5 (\Delta_u) \leftarrow \nu_4 (\Pi_g)$ is composed of two parts; the $f \leftarrow e$ component is relatively sharp and is degrading to higher frequencies, the $e \leftarrow f$ component is broad and goes to opposite direction. The latter is well resolved and could be nicely fitted (std. dev. 0.00044 cm^{-1}) although the resonance effects are large.

In the analysis of the hot bands $\nu_2 + \nu_4 + \nu_5 \leftarrow \nu_4$ the l-resonance effects are as important as above in the case of $\nu_2 + 2\nu_5 \leftarrow \nu_5$. The basic elements for the rotational l-resonance are those given by (3). In addition the vibrational l-resonance, which couples the Σ_u^+ and Σ_u^- states, must be included [1, 9]. We took into account the J dependence of the element by writing

$$r_{45} = r_{45}^0 + r_{45}^j J(J+1) . \qquad (5)$$

The diagonal elements were obtained from (2) by writing $t = 4$, $t' = 5$ and $l = l_4 + l_5 = \pm 2$ or 0. By using the symmetric and antisymmetric combinations of the initial wave functions the 4×4 matrices for every J could be reduced to pairs of 2×2 matrices. One matrix contains Σ^+ and Δ^e and the other Σ^- and Δ^f states. In the former the rotational l-resonance effects are large and in the latter they are small because the coupling elements include the sum and difference of q_4 and q_5, respectively. In the analysis the constants for the state $v_4 = 1$ were fixed and they are given in the beginning of Table 5. The fit of the upper state energies included simultaneously all 109 lines assigned in $\nu_2 + \nu_4 + \nu_5 \leftarrow \nu_4$. The resulting molecular parameters are given in Table 5. Our values for g_{45} and g_{55} as well as for r_{45}^0 and r_{45}^j are quite near to the results from the hot bands accompanying ν_5 [2]. The small differences can be attributed to the higher order terms.

Acknowledgements

The authors would like to thank Dr. J. Hietanen for useful discussions. This work has been financially supported by Academy of Finland.

[1] J. Hietanen, Acta Univ. Oulu **A 181** (1986).
[2] M. Huhanantti, J. Hietanen, R. Anttila, and J. Kauppinen, Molec. Phys. **37**, 905 (1979).
[3] E. Kyrö and R. Paso, J. Mol. Spectrosc. **110**, 164 (1985).
[4] R. Paso, Acta Univ. Oulu **A 168** (1985).
[5] G. Guelachvili, J. Mol. Spectrosc. **79**, 72 (1980).
[6] E. Kostyk and H. L. Welsh, Can. J. Phys. **58**, 912 (1980).
[7] J. Pliva, J. Mol. Spectrosc. **44**, 165 (1972).
[8] W. J. Lafferty, R. D. Suenram, and D. R. Johnson, J. Mol. Spectrosc. **64**, 147 (1977).
[9] M. Winnewisser and B. P. Winnewisser, J. Mol. Spectrosc. **41**, 143 (1972).